Bull. Astr. Soc. India (2005) **33**, 245–252

Radio astronomical imaging and phase information

Ashok K. Singal*
Astronomy & Astrophysics Division, Physical Research Laboratory, Ahmedabad, 380 009, India

Abstract. Some basic concepts in use for making astronomical observations at radio wavelengths are introduced. In particular the importance of phase information for imaging in radio astronomy is highlighted. Using simple examples it is demonstrated how phase information is much more essential than that even of amplitude for an image reconstruction from its Fourier components.

Keywords : Techniques: image processing – radio continuum: galaxies – (galaxies:) quasars: individual:1432+158

We are going to describe here in a simplified manner some concepts needed for radio astronomical observations. It is presumed that most of the astronomers attending this symposium may be more familiar with the optical and infrared techniques and might not be so familiar with the radio methods.

Figure 1 shows a grey-scale radio map of a typical AGN (3C219) observed with the VLA (Very Large Array) with an arcsec resolution. As we all know getting arcsec resolutions at radio wavelengths may need an aperture size of a few to hundreds of kilometres (depending upon the wavelength of operation). Even assuming that such a thing were really possible, there is yet another problem. Radio astronomers do not have something like a photographic plate or a CCD or NICMOS array which can be used to get a direct 2-dimensional image of a source in the sky. In general what they get from an antenna feed is an output representing total emission integrated over the whole radio source. Thus even if we were to somehow build such a large aperture, to get a 2-dimensional map this monolithic structure has to be steerable in both angular co-ordinates or it has to be a suitably designed antenna system with the capability of a complicated maneuvering of the feed in the focal plane so as to be able to collect emission from different directions in sky. For example to produce a map like that in figure 1 (a

*e-mail:asingal@prl.ernet.in

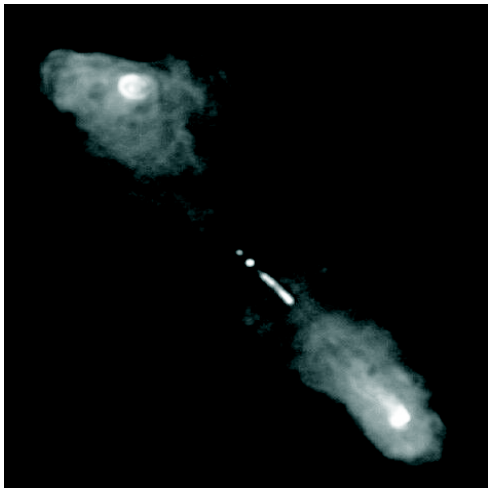

Figure 1. Radio image of 3C219.

$3' \times 3'$ field observed with $1.3'' \times 1.2''$ resolution), depending upon the exact system, it may require something like 20,000 movements of the antenna or the feed.

These difficulties in getting a direct radio image has made radio astronomers take recourse to working in the Fourier transform plane of a radio source. If $I(x, y)$ represents the source brightness in angular co-ordinates (x, y) in the sky plane, then its Fourier transform is given by,

$$F(u, v) = \int I(x, y)\, e^{-i2\pi(ux+vy)}\, \mathrm{d}x\, \mathrm{d}y \tag{1}$$

where (u, v) are the spatial co-ordinates (in units of the wavelength of operation) in a plane (usually called the uv-plane) that lies perpendicular to the line of sight towards the radio source in sky.

Figure 2 shows the 2-dimensional Fourier transform of the radio image in figure 1. Although figure 2 depicts only the amplitude part of the Fourier transform, associated with each point in this plane is also a phase information. Thus even though $I(x, y)$ is a real function, $F(u, v)$ is in general complex, having both an amplitude and a phase and it could be written as $F(u, v) = A(u, v)\, e^{i\phi(u,v)}$. Radio astronomers measure these Fourier components (also called visibilities) and then use an inverse Fourier transform,

$$I(x, y) = \int F(u, v)\, e^{i2\pi(ux+vy)}\, \mathrm{d}u\, \mathrm{d}v = \int A(u, v)\, e^{i[2\pi(ux+vy)+\phi(u,v)]}\, \mathrm{d}u\, \mathrm{d}v \tag{2}$$

to arrive at the radio image. To measure each of these Fourier components, a 2-element radio interferometer is used. One of the elements of the interferometer-pair is taken to

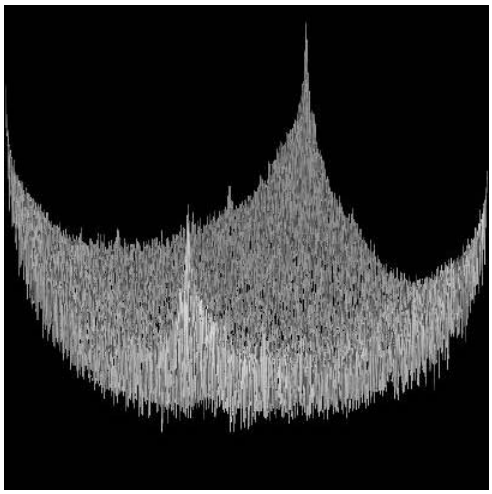

Figure 2. A 3-d surface-map representation of the 2-d Fourier transform of 3C219, with the amplitude plotted on a log scale.

be a reference antenna and is assumed to lie at the origin of the uv-plane. The baseline vector of the other element (with respect to the reference antenna) projected into the uv-plane determines the (u, v) point in the Fourier transform plane for which the interferometer yields the Fourier component (visibility). A different baseline vector between the two antennas gives Fourier component corresponding to a different (u, v) point. One can therefore cover different points in the uv-plane by making one of the elements movable (say, by putting it on rails) or one can form a large number of simultaneous interferometer pairs having different baselines by employing more number of antennas. N antennas yield $N(N-1)/2$ interferometer pairs. Radio astronomers also make use of the daily rotation of earth to cover different points in the uv-plane as the projection of an interferometer baseline in the plane normal to the line of sight to the source (i.e., the uv-plane) changes with a change in the source hour angle. By collecting sufficient number of Fourier components one can then use the invert transform to get the radio image.

Quite often people while talking of Fourier transform mean only a power spectrum (which gives square of the amplitude, i.e., $A^2(u, v)$) while the phase information for them may be unimportant. However, for imaging, phase information is essential; in fact it is much more important than that of amplitude (see e.g., Openheim and Lim 1981; Juvells et al., 1991). We will demonstrate this here using a simple example. Figure 3 shows a Fourier transform of our adopted example. Again, associated with each point is also a phase value. Differences between figures 2 and 3 may not be that apparent, however an inverse Fourier transform on figure 3 results in an image (figure 4) that appears very much different from that in figure 1. We have purposely chosen this image comprising a human face for our demonstration as any changes in such an image may be much more easily recognizable as compared to those in an abstract-looking radio map of a sky region.

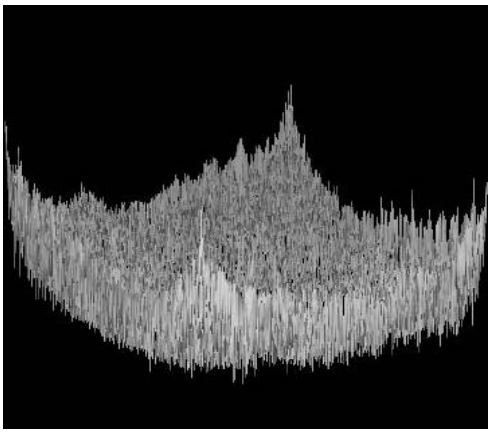

Figure 3. Fourier transform of the example-image.

Now we again do a Fourier inversion on data in figure 3, but after suppressing the phase information. Thus phase values $\phi(u,v)$ for all points in figure 3 are set equal to zero, to get

$$I_A(x,y) = \int A(u,v)\, e^{i2\pi(ux+vy)}\, \mathrm{d}u\, \mathrm{d}v\,. \tag{3}$$

The resultant image is shown in figure 5. This image shows no recognizable features and it seems to show no semblance to the original image of figure 4.

Now we repeat this exercise by keeping all the phase information intact but setting the amplitude of all Fourier components to a fixed average value A_0, to get

Figure 4. Image reconstructed from the Fourier components shown in Fig. 3, using complete amplitude and phase information.

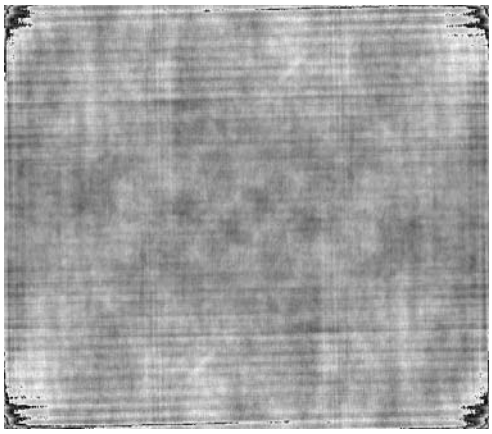

Figure 5. Image I_A reconstructed using only the amplitude information. The phase values for all Fourier components have been set equal to zero.

$$I_\phi(x,y) = A_0 \int e^{i[2\pi(ux+vy)+\phi(u,v)]}\,\mathrm{d}u\,\mathrm{d}v\,. \tag{4}$$

The resultant image (figure 6) now does appear to have a reasonable resemblance with the original image (figure 4). In I_ϕ we notice a face and many other recognizable features from the original image; all these were absent in I_A which used no phase information. It is therefore clear that phase information is totally indispensable in imaging and that for a radio astronomer a loss of phase may result in a 'loss of face' as the maps produced then may be very different from that of the actual source.

Figure 6. Image I_ϕ reconstructed using only the phase information. The amplitudes for all Fourier components have been set equal to a fixed average value.

Radio astronomers therefore, during mapping, have to pay particular attention to get accurate phase information, which tends to get corrupted due to various reasons. Cause of the phase errors may be instrumental (amplifiers, transmission lines or other electronic equipment in the signal path may each contribute their additional phase) or/and it could be due to the intervening medium between the source and the telescope. Ionosphere in particular plays the roll of a spoil-sport in this aspect. A standard practice during observations is to choose one or more phase calibrators (sources having a simple brightness distribution with known visibilities, and preferably unresolved 'point' sources) in sky regions close to the source of interest and then at some regular intervals (say, every 20-30 minutes) the actual source observations are interspersed with the observations of a phase calibrator which, depending upon the strength of the calibrator, may last for a few minutes. Assuming that ionosphere does not change too rapidly between two successive calibrations and that the sky position of the calibrating source is close enough to the source of interest (so that one sees both of them through roughly the same ionospheric patch), one can then calibrate out the phase errors caused by the ionosphere. However the non-availability of sufficient number of suitable calibrators over the sky and the occurrences of fast changes in the ionosphere may make it rather difficult to reduce the phase errors to an acceptable level. To cope up with this radio astronomers have come up with a technique called self-calibration (often abbreviated to self-cal, see e.g., Pearson and Readhead 1984) whereby most such phase errors could be taken care of. The technique works on the tacit assumption that most of the phase errors are individual antenna-based. Thus a system with N antennas at any time yields $N(N-1)/2$ visibility values (one for each interferometer pair), but these measurements have only N number of phase errors (one for each individual antenna). Now whenever there are three or more antennas in a system it is possible to find between the observed (and presumably corrupted) visibilities certain algebraic relations (called closure phase relations) which are devoid of these phase errors. These relations give us $(N-1)(N-2)/2$ constraints which when applied judiciously improve the image quality very much.

Figure 7 shows an actual record of 333 MHz observations of a calibrator (3C286) made with the GMRT (Giant Metrewave Radio Telescope). The GMRT consists of thirty 45-m antennas in an approximate 'Y' shape similar to the VLA but with each antenna in a fixed position. Twelve antennas are randomly placed within a central 1 km by 1 km square (the "Central Square") and the remainder form the irregularly shaped Y (6 on each arm) over a total extent of about 25 km. Thirty antennas of GMRT yield simultaneously 435 visibilities at any time. Further details about the array can be found at the GMRT website at `http://gmrt.ncra.tifr.res.in`.

For a 'point' calibrator like 3C286, one expects the phase vs. time plots to be horizontal straight lines. However the observed plots in figure 7 show large phase variations for all of the shown baselines; there being almost complete cycles of 360 degree phase variations in about an hour of observation time. These are particularly large variations, larger than what generally expected. But even such large phase variations mostly disappear after the self-cal technique is applied (figure 8) and the resultant plots now appear

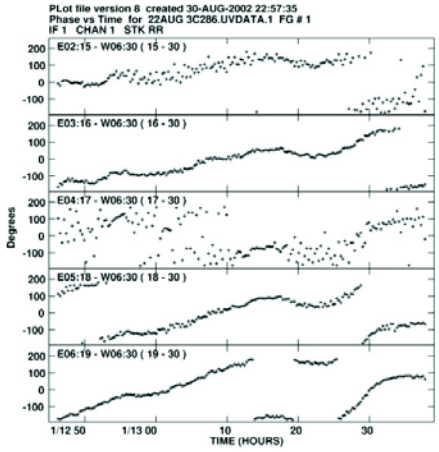

Figure 7. A sample of variation of phase across some baselines of GMRT

almost horizontal. Of course for a more complex and an unknown brightness distribution we may not have sufficient a-priori knowledge of how the uncorrupted phase plots should have looked to be sure that the scheme has worked. But experience has shown that self-cal does work in most such cases.

Figure 9 shows a 333 MHz map of a giant radio quasar, J1432+158, observed with the GMRT. It is in fact the most-distant giant quasar, which is at a redshift of 1.005. The radio source has a total angular extent of 168 arcsec, corresponding to a projected

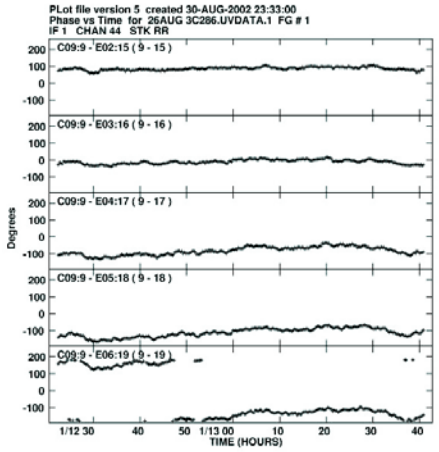

Figure 8. Variation of phase after self-cal has been applied

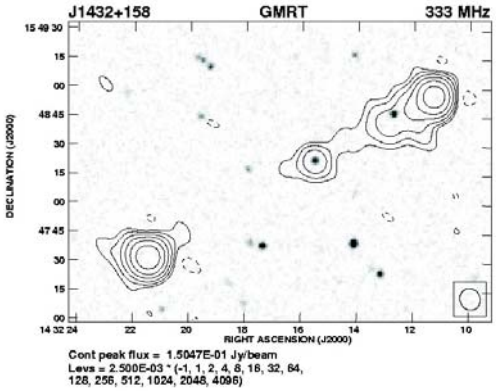

Figure 9. Radio map of J1432+158 at 333 MHz.

linear size of 1.4 Mpc. This makes it presently the largest single object observed beyond a redshift of one (Singal, Konar and Saikia 2004). During the observation of this source there were large phase variations as seen from the calibrator observations (Figure 7 and 8 records belong to the same batch of observations). We have been able to get the map in figure 9 after applying the self-cal technique, which is now almost routinely used for getting high-quality radio astronomical maps.

Acknowledgements

Grey-scale image of 3C219 was generated with data from telescopes of the National Radio Astronomy Observatory, a National Science Foundation Facility, managed by Associated Universities, Inc. The GMRT is a national facility operated by the National Centre for Radio Astrophysics of the Tata Institute of Fundamental Research.

References

Juvells, I., Vallmitjana, S., Carnicer, A. and Campos, J. 1991, *Am. J. Phys.*, **59**, 744.
Openheim, A. V. and Lim, J. S. 1981, *Proc. IEEE*, **69**, 529.
Pearson, T. J. and Readhead, A. C. S. 1984, *ARA&A*, **22**, 97.
Singal, A. K., Konar, C. and Saikia, D. J. 2004, *MNRAS*, **347**, L79.